Engineering and Technology Journal e-ISSN: 2456-3358

Volume 11 Issue 02 February-2026, Page No.-8950-8957

DOI: 10.47191/etj/v11i02.20, I.F. – 8.482

Explainable Deep Learning for Lung Disease Detection on Chest X-Ray Images Using Shapley Additive Explanations (SHAP)

Muhammad Irsyad[1], Benny Sukma Negara[2*], Sarifah Muliani[3]

[1,2,3]Informatics Engineering Study Program, Faculty of Science and Technology, Universitas Islam Negeri Sultan Syarif Kasim Riau, Pekanbaru-Riau, Indonesia.

ABSTRACT: X-ray imaging is an effective method for detecting lung diseases, such as COVID-19 and pneumonia. With the advancement of technology, the diagnosis process can now be carried out more accurately by utilizing artificial intelligence-based systems. One of the most widely used methods is deep learning, but this method is black-box, making it difficult to understand the reasons behind the model's decisions. The purpose of this study is to build an X-ray image classification system using a deep learning model based on a Convolutional Neural Network (CNN) with a VGG-16 architecture, and to apply the Shapley Additive Explanations (SHAP) method to provide explanations regarding the visuals related to the image areas that affect the prediction results. The model was trained using several configurations, and the best results were obtained with a data ratio of 80%:20%, a learning rate of 0.001, a batch size of 32, and 50 epochs. The results showed that the model was able to achieve an accuracy of 95.75% on the training data and 96.00% on the validation data. The SHAP method was used to improve understanding of the model's predictions and can display feature contributions in the form of a heatmap. This makes it easier to understand which areas have the most influence on the prediction results. The results show that the combination of deep learning and SHAP is capable of providing visual explanations for the model's prediction results.

KEYWORDS: COVID-19, Pneumonia,Citra *X-ray, Explainable Artificial Intelligence, Shapley Additive Explanations*

I. INTRODUCTION

Given the widespread impact and high mortality rate of diseases such as COVID-19 and pneumonia, they pose a serious threat to global health [1]. The year 2020 itself is even remembered as the year of COVID-19, a disease caused by the coronavirus [2]. The virus that caused this pandemic, severe acute respiratory syndrome coronavirus 2 (SARS-cov-2), first appeared in China in January 2020 [3]. Similarly, pneumonia is also a respiratory tract infection that can cause serious complications and even death, especially in vulnerable groups such as children, the elderly, and individuals with comorbidities [4]. COVID-19 and pneumonia have similar clinical symptoms, such as fever, cough, and shortness of breath, making them difficult to distinguish without supporting medical imaging tests, such as chest x-rays [5].

Although examinations such as MRI (Magnetic Resonance Imaging) and CT scans (Computed Tomography) can provide more detailed images, both methods are relatively expensive and limited in availability, especially in low-income areas [6]. The use of x-ray imaging is the most effective and relatively affordable option for detecting various lung diseases [7]. With the development of technology, particularly in the field of artificial intelligence (AI), deep learning methods have proven to be reliable in various medical imaging tasks, including x-ray image analysis [8]. This technology is capable of automatically recognizing visual patterns and producing accurate predictions, thus having great potential to assist in the diagnosis of lung diseases more quickly and efficiently [7].

Deep learning is a branch of machine learning designed to improve efficiency in processing complex data and produce more accurate prediction and classification models [9]. One deep learning architecture is the artificial neural network (ANN), which mimics the way biological neural networks process information. ANN consists of interconnected layers of neurons that are capable of learning data patterns through training [10]. One of the developments of ANN is convolutional neural network (CNN), which is designed for image data processing. In this study, CNN was used to recognize patterns in chest X-ray images to detect abnormalities with high sensitivity and specificity [11]. In this study, the CNN architecture used is the visual geometry group 16 (VGG-16), which has the ability to detect visual features through a simple but effective convolution layer arrangement [3]. Previous studies have shown that VGG-16 performs very well, not only achieving high accuracy but also having great potential for application in various image classification domains. One such study [12] used the VGG-16 architecture for fish classification and achieved an accuracy of 99.5%. In addition, a study [13] on the classification of pneumonia and COVID-19 based on x-ray images using the Deep Residual Network algorithm achieved an accuracy of 91.2%. Another study [14] compared the ability to classify lung x-ray images using transfer learning methods with resnet-50 and VGG-16, and the results showed that VGG-16 was superior in terms of accuracy.

Although deep learning models are capable of providing accurate predictions, they are black-box models, meaning that their decision-making processes are difficult for end users to understand, especially in the field of healthcare [15]. This necessitates the use of explainable AI (XAI) methods to provide a more transparent picture of the reasons behind the predictions generated [16]. The application of XAI allows for increased understanding of the model, builds user trust, and helps identify potential errors in AI systems more effectively [17]. In this study, the XAI method used is Shapley Additive Explanations (SHAP), which can assist in the interpretation of medical images [11].

Several previous studies have proven the effectiveness of the SHAP method in improving the interpretability of image-based deep learning models. In addition, the study compared several transfer learning methods, such as EfficientNetB0, InceptionV3, and LetNet, with an accuracy of 99.20%. The study stated that the SHAP and LIME methods were able to provide important insights into the model's decision-making process, while Grad-CAM and Grad-CAM++ highlighted the image areas that contributed to the classification results [18]. Another study also applied the transfer learning method using the Xception model and achieved an accuracy of 98.2%. In addition, the study utilized the Grad-CAM and SHAP techniques to provide a visual explanation of the AI prediction process, thereby increasing understanding and trust among medical personnel [7].

Based on previous research, the SHAP method has been proven to provide local interpretations of model predictions by showing the contribution of each feature to the classification results [19]. The model-agnostic nature of SHAP allows it to be applied to various deep learning architectures, making it flexible for medical image interpretation. This study applied SHAP to improve model transparency and support the decision-making process [20].

The scope of this study is limited to the process of interpreting prediction results, namely using the Shapley Additive Explanations (SHAP) method to provide visual explanations of the image areas that influence the model's decisions.

1. This study utilizes chest x-ray images as the main data source to classify three categories of lung conditions, namely COVID-19, pneumonia, and normal. In the classification system development process, the deep learning model used is limited to the Convolutional Neural Network (CNN) VGG-16 architecture without involving other architectures for comparison.
2. The process of interpreting the prediction results in this study was carried out by applying the Shapley Additive Explanations (SHAP) method, which serves to display a visualization of the areas in the image that contribute to the model's classification decision.

II. METHODOLOGY

The research method stages in this study consist of several processes, starting from the data collection stage, followed by data preprocessing, deep learning, model performance evaluation, and finally the implementation of explainable AI (XAI) using Shapley additive explanations (SHAP) to provide interpretations of the prediction results.

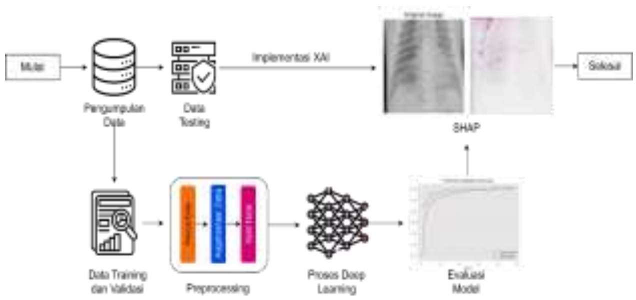

Figure 1. Research Stages

2.1 Data Collection

In this study, the dataset collected came from a public dataset consisting of three classes, namely COVID-19, normal, and pneumonia. In total, there were 3,030 chest x-ray images divided into training data and testing data, where the training data consisted of 3,000 x-ray images obtained from the Mendeley website [21]. Meanwhile, the testing data consists of 10 X-ray images per class taken from the same site, but never used or seen by the model during the training process. Each class in the testing data consists of 10 X-ray images, so it can be used to test the model's ability to make predictions on new data.

Figure 2. COVID-19

Figure 3. Normal

Figure 4. Pneumonia

2.2 Data Pre-processing

At this stage, a series of preprocessing steps are carried out to prepare the x-ray images before they are used in the deep learning model training process. This process is important to ensure that the data used is in a standard condition and in the format required by the model architecture. Several preprocessing steps are carried out, including loading images and their labels, resizing images, augmenting data, and dividing the dataset into training data and validation data

2.2.1 Resize

After all images have been successfully loaded, the next step is to resize them to 224 x 224 pixels. This size was chosen because it matches the input format required by the VGG-16 architecture. This size adjustment was done to ensure that all images have the same dimensions, thereby minimizing errors during the training process.

2.2.2 Data Augmentation

Next, data augmentation is performed to add image variation. The augmentation technique used is a rotation range of 10 degrees with the nearest interpolation method. This process aims to enable the model to adapt to differences in image orientation. In addition, rescalling was performed on the images to a scale of 1/255 to adjust the pixel value range to 0 to 1, which is the standard input for deep learning models [18].

2.2.3 Data Split

Next, the data split process was carried out by dividing the training data and validation data. This division was done to ensure a balanced data distribution in each category. The training and validation data were separated based on the deep learning stages with several ratios, namely 70% training data and 30% validation data, 80% training data and 20% validation data, and 90% training data and 10% validation data. Several tests were conducted to determine the data distribution ratio that provided the best performance for the model. The test results can be seen in Table 2

2.3 Deep Learning Process

The deep learning process is applied using a convolutional neural network (CNN) algorithm with the Visual geometry group-16 (VGG-16) architecture [3]. This architecture was chosen because it is widely used in various image classification studies and has proven to perform well. VGG-16 has 13 convolution layers, followed by 5 pooling layers and 3 fully connected layers at the end [22]. All convolution layers in VGG-16 use a 3x3 kernel with padding 1 and stride 1, enabling them to capture visual features in detail [23]. In this study, the deep learning process consists of two stages, namely model building and model training.

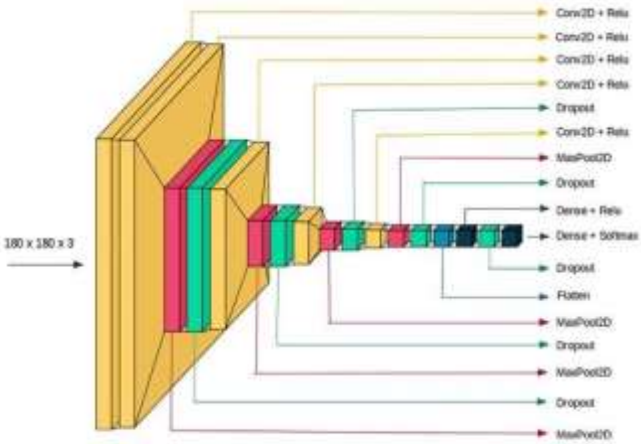

Figure 5. VGG-16 Architecture

2.3.1 Model Development

At this stage, the deep learning model was developed using the VGG-16 architecture as the base model. VGG-16 was loaded without a fully connected layer, and several classifier layers were added on top of it, namely the AveragePooling2D layer to convert the output from a matrix into a one-dimensional vector. Next, a Danse layer with 64 neurons is added and activated using the ReLU activation function. A dropout layer of 0.5 is inserted as the output layer to reduce the risk of overfitting, then a Danse layer with 3 units is used in accordance with the number of classes: COVID-19, normal, and pneumonia. It is activated using the softmax activation function to produce probabilities for each class. Next, the entire layer in the base model is frozen so that the pretrained weights from ImageNet are not updated during the training process. The model is then compiled using the Adam optimizer, loss function, and accuracy matrix.

2.3.2 Model Training

After the model was built, the training process was carried out using the Adam optimizer with various learning rate variations, namely 0.1, 0.01, 0.001, 0.0001, and 0.00001. In addition, tests were conducted on combinations of epoch parameters of 20, 30, and 50, as well as batch sizes of 8, 16, and 32. The purpose of varying these parameters was to find the best combination that could produce optimal performance in the classification process.

2.4 Model Evaluation

After training the model, it is evaluated using a classification report that displays precision, recall, f1-score, and accuracy for each class. In addition, the model's performance is visualized in the form of a confusion matrix to describe in more detail how accurately the model classifies chest x-ray images into three classes [24]. The evaluation matrix values are obtained using the following formula:

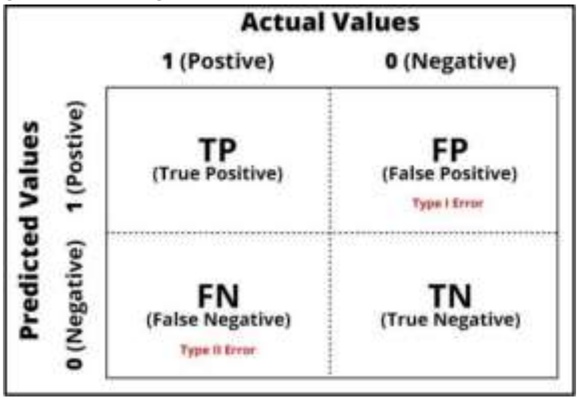

Figure 6. Confusion Matrik

$$Accuracy = \frac{TP + TN}{TP + TN + FP + FN}$$

$$Precision = \frac{TP}{TP+FP}$$

$$Recall = \frac{TP}{TP + FN}$$

$$F1 - score = 2 \text{ x } \frac{Precision \text{ x } Recall}{Precision + Recall}$$

Keterangan :
TP = Jumlah data positif yang diklasifikasibenar.
TN = Jumlah data negatif yang diklasifikasi benar.
FP = Jumlah data positif yang diklasifikasi salah.
FN = Jumlah data negatif yang diklasifikasi salah

2.5 XAI Implementation

In this study, the Explainable AI (XAI) method was applied to provide explanations for the prediction results of deep learning models that are black-box or inexplicable [16]. The implementation of XAI aims to improve the transparency and interpretability of prediction results, so that users such as doctors or medical personnel can understand the reasons behind the decisions made by the model [18]. One of them is using the Shapley Additive Explanations (SHAP) method, which can show how much each feature contributes to the model's decision.

2.5.1 Shapley Additive explanations (SHAP)

Shapley Additive Explanations (SHAP) is an explainability technique introduced by Lundberg and Lee [20]. The basic concept of this method comes from the Shapley value, which was first introduced by Lloyd Shapley in 1953 with cooperative theory [19]. SHAP is included in the explainable AI (XAI) method, which can explain the contribution of each feature to the model prediction [18]. The Shapley value from game theory forms the basis for calculating contribution values in the SHAP method, thereby explaining the extent of each feature's influence in the decision-making process [25]. The formula for calculating the Shapley value is as follows:

$$\varphi j(v) = \varphi j = \sum_{S \subseteq M \setminus \{j\}} \frac{|S|!\,(M - |S| - 1)!}{M!} \left(v(S \cup \{j\}) - v(S)\right)$$

Explanation:
M = set of all features in the model.
S = subset of features without feature j.
f (S) = model prediction value when only features in S are used.
f $(S \cup \{j\})$ = the model's prediction value when feature j is added to subset S
$\frac{|S|!(M-|S|-1)!}{M!}$ = is the probability weight that a subset S is selected in the calculation

The SHAP implementation process to explain the prediction results of a *deep learning* model based on chest *x- ray* images is carried out through the following stages

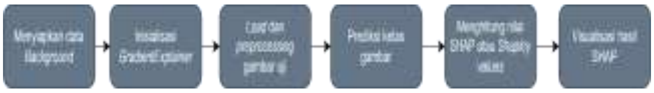

Figure 7. Proses Implementasi SHAP

Preparing background data
Background data is a collection of images from the validation dataset used as a baseline in the SHAP value calculation process. This data is loaded using ImageDataGenerator with pixel normalization to a scale of 0-1, then several batches of images are taken to be used as background.

1. Initializing GradientExplainer

Once the background data is ready, the next step is to initialize the explainer using GradientExplainer from the SHAP library. This explainer requires a trained deep learning model and background data as a reference in calculating the prediction baseline [18].

3. Loading and preprocessing test images

The test images to be analyzed are loaded from the storage directory, then converted into arrays, resized to 224x224 pixels, and normalized to a scale of 0-1 to match the deep learning model input format.

4. Predicting image classes

The processed test images are then predicted using the model. The prediction results are in the form of probability values for each class, and the class with the highest probability is selected as the final prediction result.

5. Calculating SHAP values

SHAP values are calculated using the explainer.shap.values() function. These values show how much each pixel contributes to the prediction generated by the model for each class.

6. Visualizing SHAP results

The calculated SHAP values are then visualized in the form of a heatmap using Matplotlib. This heatmap displays the original image along with a map of pixel contributions to each class. Red indicates areas with positive contributions to the pixel, while blue indicates negative contributions [18].

III. RESULTS AND DISCUSSION

In this study, a series of experiments were conducted with several testing scenarios used to evaluate model performance. Each scenario used different training parameters, dataset splits, optimizer types, activation functions, learning rate values, batch sizes, and number of epochs. The purpose of these experiments was to find the best configuration capable of providing optimal performance in classifying chest x-ray images into three categories: COVID-19, normal, and pneumonia.
Table 1 shows the list of training parameters used in this study. The parameters include the data split ratio, number of epochs, learning rate, and batch size. The optimizer used is Adam with the ReLU activation function in all experiments.

Table 1. Model training parameters

Parameter	Nilai
Pembagian data	70% : 30%, 80% : 20%, 90% : 10%
Optimizer	Adam
EPOCH	20, 30, dan 50
Activation Function	ReLU
Batch Size	8, 16, dan 32
Learning Rate	0.1, 0.01, 0.001, 0.0001, 0.00001

After the model was trained using different combinations of parameters, the results of accuracy, loss values, validation accuracy, and validation loss values were obtained for each test scenario. The results of each combination can be seen in Table 2 below.

Table 2. All test results

	Rasio	Learning Rate	EPOCH	Batch Size	Accuracy	Val Accuracy	Loss	Val Loss
1	70%:30%	0.1	20	8	34.88	33.11	1.1176	1.1034
2	70%:30%	0.01	30	16	82.13	93.33	0.4134	0.1934
3	70%:30%	0.001	50	32	94.04	93.12	0.1935	0.1813
4	70%:30%	0.0001	30	32	85.3	87.71	0.4326	0.3694
5	70%:30%	0.00001	30	32	59.23	79.32	0.2994	0.8738
6	80%:20%	0.1	20	8	34.18	33.33	1.1067	1.1094
7	80%:20%	0.01	30	16	82.97	91.67	0.4084	0.2885
8	**80%:20%**	**0.001**	**50**	**32**	**95.75**	**96.00**	**0.1408**	**0.1175**
9	80%:20%	0.0001	30	32	86.18	87	0.4296	0.3673
10	80%:20%	0.00001	50	32	68.11	80.83	0.8335	0.7657
11	90%:10%	0.1	20	8	32.41	33.33	1.1072	1.1027
12	90%:10%	0.01	30	16	85.99	93.11	0.3573	0.2341
13	90%:10%	0.001	50	32	93.27	94.52	0.2089	0.1663
14	90%:10%	0.0001	30	32	86.38	89.93	0.4162	0.3279
15	90%:10%	0.00001	30	32	57.26	77.67	0.9185	0.8494

Based on Table 2, it can be seen that the model with a ratio of 80%:20% with a learning rate of 0.001, batch size of 32, and number of epochs of 50. The highest validation accuracy value was obtained in the configuration with a ratio of 80%:20%, namely 96.00% with a validation loss value of 0.1175%. Conversely, the model with a learning rate of 0.1 produced very low accuracy in all scenarios, ranging from 33-34%, both in the training and validation data. This shows that a learning rate that is too large can cause the model learning process to become unstable. In addition to using tables, the training and validation results of the model are visualized in graph form to facilitate analysis. Figure 7 shows a graph of changes in accuracy and loss values during the training process.

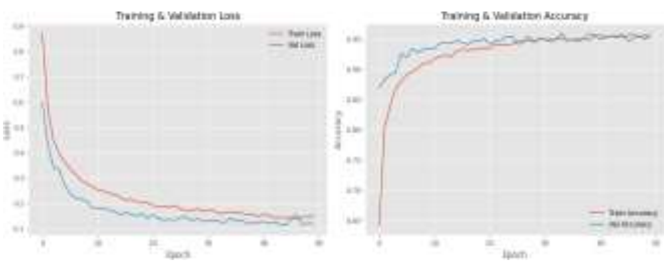

Figure 8. Accuracy chart

The image above shows that the accuracy of the training and validation data both increased to 90%. The loss value also continued to decline and stabilized below 0.2 after passing the 20th epoch. The results show that the model learns well without overfitting, as the training and validation performance are balanced until the end of the 50th epoch. In addition to the accuracy graph, testing was carried out using numerical evaluation matrices such as precision, recall, and

F1-score to determine the model's performance in classifying each class. The results can be seen in Table 3.

Table 3. Classification Report

	Precision	Recall	F1-Score	Support
COVID-19	97	99	98	200
Normal	93	97	95	200
Pneumonia	98	92	95	200
Accuracy			96	600

In addition to using numerical evaluation matrices such as precision, recall, and F1-score, an analysis was also conducted using a confusion matrix to see the number of correct and incorrect predictions in each class. The following image is a confusion matrix of the best model prediction results:

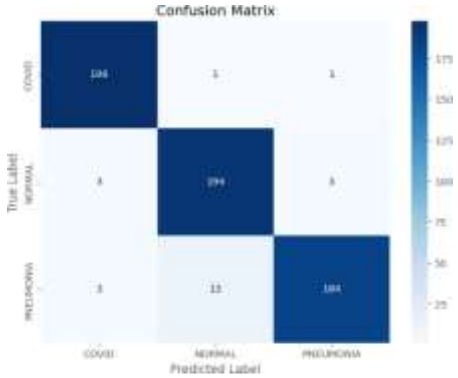

Figure 9. Confusion Matrix

Based on the confusion matrix above, it can be seen that for the COVID-19 class, 198 predictions were correct, while 1 data was incorrectly predicted as normal, and 1 as pneumonia. In the normal class, there were 194 data that were predicted correctly, 3 data were incorrectly predicted as COVID-19, and 3 data were incorrectly predicted as pneumonia. Meanwhile, the pneumonia class successfully predicted 184 correct predictions, 3 data incorrectly predicted as COVID-19, and 13 data incorrectly predicted as normal

In addition to evaluating model performance using a numerical matrix and confusion matrix, this study also interpreted the prediction results using the Shapley Additive Explanations (SHAP) method to provide a visual overview of the contribution of each pixel to the prediction results generated by the model. The interpretation process was carried out by applying SHAP to the best model, namely the model with a data ratio of 80%:20%, a learning rate of 0.001, a batch size of 32, and 50 epochs. The SHAP visualization results are displayed in the form of a heatmap, where red indicates pixels that contribute positively to the class prediction, while blue indicates negative or insignificant contributions. The color bar at the bottom of the image shows the range of SHAP values generated, from -0.01 to 0.01. Positive values on the right are marked with a gradation from white to red, while negative values on the left are marked with a gradation from white to blue. The closer the value is to 0, the whiter the color displayed, which means that the pixels in that area are neutral and do not have a significant influence on the model's decision.

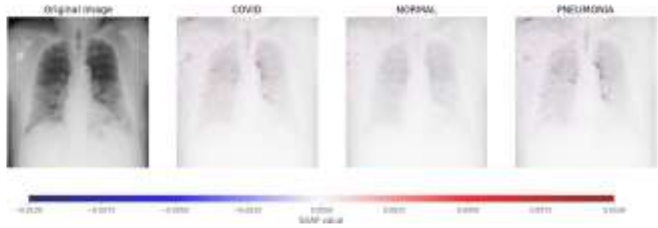

Figure 10. Based on the highest SHAP value in the second column, the x-ray image was diagnosed with COVID-19.

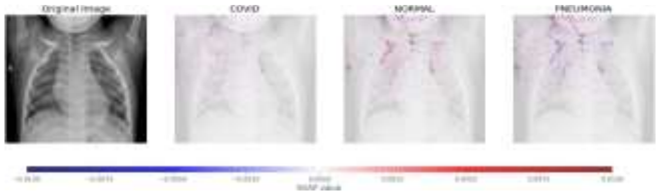

Figure 11. Based on the highest SHAP value in the second column, the x-ray image was diagnosed with COVID-19.

Overall, the use of SHAP in this study was able to provide a clear picture of how the model makes decisions. The resulting heatmap visualization shows that the important areas in the image correspond to the model's prediction results. Therefore, this interpretation method can be an additional support in the development of deep learning-based decision systems, especially in the medical field.

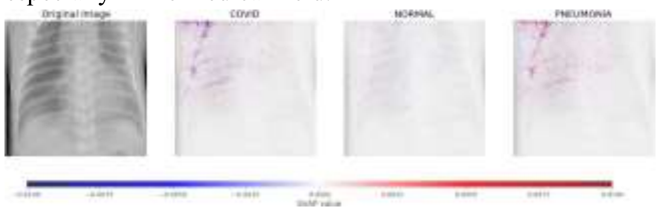

Figure 12. Based on the highest SHAP value in the second column, the x-ray image was diagnosed with Pneumonia

4. CONCLUSION

The results of this study indicate that the deep learning model using the VGG-16 architecture is effective in classifying chest x-ray images to detect COVID-19, normal conditions, and pneumonia. The model showed the best performance at a data ratio of 80%:20%, using the Adam optimizer, a learning rate of 0.001, 50 epochs, and a batch size of 32. With this configuration, the model achieved a training accuracy of 95.75% and a validation accuracy of 96.00% without any indication of overfitting. Additionally, the application of the SHAP method successfully provided informative heatmap visualizations, with important areas in the images aligning with the model's prediction results. In further research, it is recommended to conduct validation tests of the SHAP method's results directly with medical personnel, specifically radiologists, to assess its benefits in supporting the diagnosis process.

REFERENCES

1. A. A. D. Halim and S. Anraeni, “Analisis Klasifikasi Dataset Citra Penyakit Pneumonia menggunakan Metode K-Nearest Neighbor (KNN),” *Indones. J. Data Sci.*, vol. 2, no. 1, pp. 01–12, 2021, doi: 10.33096/ijodas.v2i1.23.
2. A. Kumar *et al.*, “Wuhan to World: The COVID-19 Pandemic,” *Front. Cell. Infect. Microbiol.*, vol. 11, no. March, pp. 1–21, 2021, doi: 10.3389/fcimb.2021.596201.
3. S. Sharma and K. Guleria, “A Deep Learning based model for the Detection of Pneumonia from Chest X-Ray Images using VGG-16 and Neural Networks,” *Procedia Comput. Sci.*, vol. 218, pp. 357–366, 2022, doi: 10.1016/j.procs.2023.01.018.
4. M. Bhandari, T. B. Shahi, B. Siku, and A. Neupane, “Explanatory classification of CXR images into COVID-19, Pneumonia and Tuberculosis using deep learning and XAI,” *Comput. Biol. Med.*, vol. 150, no. September, 2022, doi: 10.1016/j.compbiomed.2022.106156.
5. N. Umzubongile, S. Mandindi, H. Vadapalli, and A. Mathematics, “Detecting and Understanding COVID-19 Misclassifications : A Deep Learning and Explainable AI Approach,” no. August, 2023.
6. M. Bhandari, T. Bahadur, B. Siku, and A. Neupane, “Explanatory classification of CXR images into COVID-19 , Pneumonia and Tuberculosis using deep learning and XAI,” *Comput. Biol. Med.*, vol. 150, no. October, p. 106156, 2022, doi: 10.1016/j.compbiomed.2022.106156.
7. A. V. Ikechukwu, “Leveraging Transfer Learning for Efficient Diagnosis of COPD Using CXR Images and Explainable AI Techniques,” *Intel. Artif.*, vol. 27, no. 74, pp. 133–151, 2024, doi: 10.4114/intartif.vol27iss74pp133-151.
8. J. Yopento, E. Ernawati, and F. F. Coastera, “Identifikasi Pneumonia Pada Citra X-Ray Paru-Paru Menggunakan Metode Convolutional Neural Network (CNN) Berdasarkan Ekstraksi Fitur Sobel,” *Rekursif J. Inform.*, vol. 10, no. 1, pp. 40–47, 2022, doi: 10.33369/rekursif.v10i1.17247.
9. R. A. Tilasefana and R. E. Putra, “Penerapan Metode Deep Learning Menggunakan Algoritma CNN Dengan Arsitektur VGG NET Untuk Pengenalan Cuaca,” *J. Informatics Comput. Sci.*, vol. 05, no. 1,pp. 48–57, 2023.
10. M. Adil, R. Ullah, S. Noor, and N. Gohar, “Effect of number of neurons and layers in an artificial neural network for generalized concrete mix design,” *Neural Comput. Appl.*, vol. 8, pp. 1–9, 2020, doi: 10.1007/s00521-020-05305-8.
11. M. A. Sufian *et al.*, “AI-Driven Thoracic X-ray Diagnostics: Transformative Transfer Learning for Clinical Validation in Pulmonary Radiography,” *J. Pers. Med.*, vol. 14, no. 8, 2024, doi: 10.3390/jpm14080856.
12. I. M. R and T. M. Johan, “Klasifikasi Citra Ikan Menggunakan Algoritma Convolutional Neural Network dengan Arsitektur VGG-16,” vol. 4, no. 2, pp. 978–985, 2023, \ doi: 10.30865/klik.v4i2.1209.
13. P. P. Illahi, H. Fauzi, and T. S. Siadari, “Klasifikasi Penyakit Pneumonia Dan Covid-19 Berbasis Citra X-Ray Menggunakan Arsitektur Deep Residual Network Classification Of Pneumonia And Covid-19 Based On X-Ray Images Using The Deep Residual Network Architecture,” vol. 9, no. 4, pp. 1837–1843,2022,[Online].Available: https://openlibrarypublications.telkomuniversity.ac.id/index.php/engineering/article/view/18232
14. T. Berliani *et al.*, “Perbandingan Kemampuan Klasifikasi Citra X-ray Paru-paru menggunakan Transfer Learning ResNet-50 dan VGG-16 VGG-16 Transfer Learning,” vol. 5, no. 2, pp. 123–135, 2023.
15. R. Rajpoot, M. Gour, S. Jain, and V. B. Semwal, “Integrated ensemble CNN and explainable AI for COVID-19 diagnosis from CT scan and X-ray images,” *Sci. Rep.*, vol. 14, no. 1, pp. 1–21, 2024, doi: 10.1038/s41598-024-75915-y.
16. P.-D. Arsenault, S. Wang, and J.-M. Patenande, “A Survey of Explainable Artificial Intelligence (XAI) in Financial Time Series Forecasting,” vol. 1, no. 1, pp. 1–35, 2024, [Online]. Available: http://arxiv.org/abs/2407.15909
17. S. Walia, K. Kumar, S. Agarwal, and H. Kim, “Using XAI for Deep Learning-Based Image Manipulation Detection with Shapley Additive Explanation,” *Symmetry (Basel).*, vol. 14, no. 8, 2022, doi: 10.3390/sym14081611.
18. E. Mahamud, N. Fahad, M. Assaduzzaman, S. M. Zain, K. O. M. Goh, and M. K. Morol, “An explainable artificial intelligence model for multiple lung diseases classification from chest X-ray images using fine-tuned transfer learning,” *Decis. Anal. J.*, vol. 12, no. July, p. 100499, 2024, doi: 10.1016/j.dajour.2024.100499.
19. H. Sahlaoui, E. A. A. Alaoui, A. Nayyar, S. Agoujil, and M. M. Jaber, “Predicting and Interpreting Student Performance Using Ensemble Models and Shapley Additive Explanations,” *IEEE Access*, vol. 9, pp. 152688–152703, 2021, doi: 10.1109/ACCESS.2021.3124270.

20. S. M. Lundberg and S. I. Lee, “A unified approach to interpreting model predictions,” *Adv. Neural Inf. Process. Syst.*, vol. 2017-Decem, no. Section 2, pp. 4766–4775, 2017.
21. doi: 10. 17632/dvntn9yhd2. . Kumar, Sachin (2022), “Covid19-Pneumonia-Normal Chest X-Ray Images”, Mendeley Data, V1, “Covid19-Pneumonia-Gambar Rontgen Dada Normal.”
22. M. Yaseliani, A. Z. Hamadani, A. I. Maghsoodi, and A. Mosavi, “Pneumonia Detection Proposing a Hybrid Deep Convolutional Neural Network Based on Two Parallel Visual Geometry Group Architectures and Machine Learning Classifiers,” *IEEE Access*, vol. 10, pp. 62110–62128, 2022, doi: 10.1109/ACCESS.2022.3182498.
23. D. K. Jain *et al.*, “Deep Learning-Aided Automated Pneumonia Detection and Classification Using CXR Scans,” *Comput. Intell. Neurosci.*, vol. 2022, 2022, doi: 10.1155/2022/7474304.
24. M. Vakili, M. Ghamsari, and M. Rezaei, “Performance Analysis and Comparison of Machine and Deep Learning Algorithms for IoT Data Classification,” 2020, [Online]. Available: http://arxiv.org/abs/2001.09636
25. T. Chrysoula and I. M. Systems, “Explainable Artificial Intelligence for Deep Learning Methods in Chest X-Ray Classification,” no. February, 2023